Reactions of Hyperthermal C(^{3}P) Generated by Laser Ablation with H_2, HCl, HBr, and CH_3OH

M. R. Scholefield, S. Goyal, J.-H. Choi, and H. Reisler*

Department of Chemistry, University of Southern California, Los Angeles, California 90089-0482

Received: May 10, 1995[⊗]

The reactions of C(^{3}P) with H_2, HCl, HBr, and CH_3OH(D) were investigated in a crossed-beam configuration using laser ablation of graphite as the source of C(^{3}P). Upon pulsed irradation of graphite with focused laser output at 266 and 355 nm, hyperthermal C(^{3}P) is produced and expands freely into the vacuum. In this "free ablation" mode, directional beams of monomeric carbon are produced with a peak velocity of ~8000 m s^{-1} and a broad velocity distribution that can be described by temperatures of ~21 000 and ~9500 K when using 266 and 355 nm ablation wavelengths, respectively. Using 266 nm ablation, the endothermic reactions of C(^{3}P) with the title molecules were investigated by probing the CH product. CH is produced predominantly in $v = 0$ with rotational distributions that are well described by temperatures in the range 1500−2200 K, depending on the molecular reactants. The spin−orbit and Λ-doublet sublevels are equally populated. In reactions with CH_3OD, both CH and CD are detected, identifying both the methyl and the hydroxyl groups as reactive sites. Comparisons with the CH internal energy distributions obtained in the reaction of C(^{1}D) with H_2 show remarkable similarities. On the basis of theoretical investigations and the known electronic states of the methylene intermediate, it is suggested that the reactions of both C(^{3}P) and C(^{1}D) proceed via insertion involving carbene intermediates. The participation of several low-lying states of the carbenes may lead both to lowering of the activation barrier for insertion and to CH products with similar populations of the two Λ-doublet components.

I. Introduction

Detailed studies of the reactions of hydrogen and second-row atoms with small molecules have provided the foundation upon which our understanding of reaction dynamics is based.[1] Conspicuous in their absence are studies of the reaction dynamics of atomic carbon in its ground electronic state, ^{3}P. Although several exothermic reactions with oxidizers (e.g., NO, N_2O) have been studied and nascent product distributions have been reported,[2−5] studies of H atom-transfer reactions are scarce; in fact, observation of the CH product has been reported only in the exoergic reaction with HI.[6] Likewise, few reactions of C(^{1}D) have been studied so far.[7−10] The absence of a substantial body of work on reactions of C(^{3}P) is of course the result of difficulties in producing atomic carbon cleanly and efficiently, as well as the endothermicity of many of its reactions with H-containing molecules. As a result, very little information on the mechanisms of these reactions and their activation barriers is available. Since CH radicals play an important role in hydrocarbon combustion,[11] studies of reactions of carbonaceous species that can yield CH under conditions relevant to high-temperature environments are desirable. In addition, atomic carbon, with only six electrons, is a good candidate for theoretical studies of its reactions with small molecules, as the recent detailed study of the C + H_2 system has demonstrated.[12] Atomic carbon is also the smallest species that can engage in insertion, addition, and abstraction reactions, which are among the most common reaction mechanisms in organic chemistry, while the availability of two low-lying spin states, ^{3}P and ^{1}D, should enable the exploration of spin-specific reactivities.[13] Thus, experimental difficulties notwithstanding, studies of reaction dynamics of atomic carbon should provide new mechanistic insights and allow detailed comparisons with theory.

It is with these goals in mind that we have developed a beam source of hyperthermal C(^{3}P) which exploits the free ablation of graphite. Although we have used graphite ablation before as a source of C(^{3}P),[2,3] we give here a full account of the source performance, using direct detection of carbon for characterization of the ablated species. We also report our first studies of the H-transfer reactions:[14]

$$C(^3P) + H_2 \rightarrow CH + H \qquad \Delta H = 1.00\ \text{eV} \quad (1)$$

$$C(^3P) + HBr \rightarrow CH + Br \qquad \Delta H = 0.27\ \text{eV} \quad (2)$$

$$C(^3P) + HCl \rightarrow CH + Cl \qquad \Delta H = 0.95\ \text{eV} \quad (3)$$

$$C(^3P) + CH_3OH(D) \rightarrow CH + CH_2OH \qquad \Delta H = 0.56\ \text{eV} \quad (4)$$

$$\rightarrow CH + CH_3O \qquad \Delta H = 0.99\ \text{eV}$$

$$\rightarrow CD + CH_3O$$

Since these reactions are endoergic, the use of the free ablation source, which generates C(^{3}P) with translational energies in the range 0.5−10 eV, is essential. We demonstrate that H-transfer pathways yielding CH radicals exist for reactions 1−4 and that translational energy can be used to enhance reactivity.

In a previous report we have suggested that the reactions of atomic carbon may be different from those of atomic oxygen in that they may involve the participation of carbene intermediates with *several* low-lying singlet and triplet states that can undergo surface crossings.[7] Such crossings can rationalize, for example, the absence of significant Λ-doublet preferences in the reactions C(^{1}D) + H_2 and C(^{1}D) + HCl.[7] The relevant surface crossings have recently been identified theoretically for the C(^{3}P) + H_2 reaction and were shown to be responsible for the reduction of the activation barrier in the entrance channel to the CH_2 insertion intermediate.[12,15,16] We suggest that similar

[⊗] Abstract published in *Advance ACS Abstracts*, September 1, 1995.

0022-3654/95/2099-14605$09.00/0

surface crossings may be important in insertion reactions of $C(^3P)$ with other H-containing molecules as well and that these reactions may have much smaller entrance channel barriers than the corresponding reactions of $O(^3P)$.

II. Experimental Section

The crossed-beam apparatus consists of an octagonal reaction chamber, a molecular beam source chamber, and an ablation chamber containing the carbon source. These are pumped separately by two 6 in. diffusion pumps and a 4 in. diffusion pump, respectively. For the data presented here, only the ablation chamber is differentially pumped (through a 3 mm skimmer). Average background pressures with both beams on are approximately 7×10^{-5} Torr, when operating at 10 Hz. A more detailed description of the ablation apparatus has been given in a previous publication.[2,3]

H_2, HBr, HCl, and $CH_3OH(D)$ molecular reactants are expanded through a pulsed nozzle (General Valve, 1 ms fwhm, 0.8 mm diameter) at a typical stagnation pressure of 760 Torr. To obtain adequate signal-to-noise (S/N) ratios, a high concentration of reactant molecules is required in the neutral beam. Thus, neat H_2, HCl, and HBr are used in the expansion, while the $CH_3OH(D)$ beam is generated by bubbling He through the alcohol heated to 52 °C in a water bath to obtain an approximately 50% $CH_3OH(D)$/He mixture. The pulsed valve is maintained at 120 °C to reduce clustering of the molecular reactant.[17] Typically, the nozzle is set at a distance of 30 ± 1 mm away from the reaction center. A series of scans taken at various stagnation pressures (ranging from 300 to 760 Torr) and nozzle distances have confirmed that relaxation in the product distributions is minimal and that clusters, if present, do not alter the product distributions.

The atomic carbon beam is generated by free laser ablation of a spectroscopic-grade graphite rod (Bay Carbon, Inc.).[18-24] The free ablation produces a hyperthermal pulsed atomic beam of short temporal duration (~5 μs fwhm at a 60 mm distance from the rod) and is also advantageous in that near complete destruction of cluster species is achieved at moderate laser fluences. For the crossed-beam studies, typically 4 mJ of 266 nm radiation from a Nd:YAG laser (Spectra-Physics GCR-11-3, 7 ns) is focused by a 50 cm focal length lens to a spot size of ~0.5 mm (2 J/cm^2 laser fluence) on, or slightly before, the graphite rod surface. The exact location of the focal point is adjusted to maximize monomeric carbon and minimize C_2 and C_3 formation. The rod is maintained in constant helical motion to ensure good shot-to-shot stability, and the uniform energy profile of the Nd:YAG laser beam leads to an efficient production of predominantly monomeric, ground state carbon, $C(^3P)$ (see section III). In the free ablation arrangement, the laser beam enters the reaction chamber through a port opposite the carbon beam skimmer, hitting the rod which has its center aligned with the laser beam. The ablated material then freely expands into the interaction chamber. The rod is placed at a distance of 60 ± 3 mm from the reaction center and ~10 mm from the carbon beam skimmer.

$C(^3P)$ is detected by two-photon laser induced fluorescence (LIF),[25] using a Nd:YAG laser pumped dye laser system (Quanta Ray DCR-1A + PDL-1). The 560 nm output of the dye laser (operating on Rhodamine 6G dye) is frequency-doubled in a KDP crystal to obtain approximately 4.5 mJ of 280 nm radiation. The laser output is then focused by a 25 cm focal length lens into the center of the freely expanding ablation plume 6 μs after the ablation pulse. Excitation of atomic carbon is achieved by two-photon absorption via either the $^3P_{J'} \leftarrow {}^3P_{J''}$ transition[25a] (~280 nm) or the $^3D_{J'} \leftarrow {}^3P_{J''}$ transition[25b] (~287 nm), and the resulting vacuum-ultraviolet (VUV) fluorescence at ~166 nm is detected at right angles to the excitation beam. We have also attempted to detect $C(^1D)$ LIF signals following two-photon excitation via the $^1P_2 \leftarrow {}^1D_2$ transition (284.2 nm);[25b] however, no signal was observed. The $C(^3P)$ fluorescence is imaged through a MgF_2 window and focused with a 25 cm focal length CaF_2 lens onto the photomultiplier tube (PMT, CsI, Hamamatsu R1259). The PMT housing is continually flushed with N_2 when recording spectra to avoid attenuation of the VUV fluorescence. Atomic carbon time-of-flight (TOF) data are subsequently collected by tuning to individual $C(^3P)$ spectral lines at 280.27 or 286.89 nm and recording the LIF signal as a function of the ablation−probe delay, at a fixed distance between the graphite rod and the excitation laser of 60 mm. TOF data are obtained for 266 nm ablation at energies of 2 and 4 mJ and for 355 nm ablation at energies of 5, 10, and 15 mJ.

$CH(X^2\Pi)$ is detected via LIF using the $B^2\Sigma^- \leftarrow X^2\Pi$ transition.[26] Although the $B \leftarrow X$ system is predissociative (at $N' = 17$ for $v' = 0$ and $N' = 9$ for $v' = 1$), it is easier to analyze than the $A^2\Delta \leftarrow X^2\Pi$ system because it has fewer branches. The $A \leftarrow X$ system is not predissociative, but it is spectrally congested and prone to rotational line overlap. It has only been used in measurements of Λ-doublet populations, since the Λ-doublet components at higher N'' states can be resolved for single R-branch lines.[26,27] To frequency calibrate our dye laser for CH detection, $CH(X^2\Pi)$ was first prepared by the two-photon photolysis of CH_3I at 266 nm, and spectra were recorded for the $B \leftarrow X$ system at ~390 nm. CH $B \leftarrow X$ line assignments are based on comparisons with these experimental line positions, as well as with published data.[26] An excimer laser pumped dye laser system (Questek 2220M, Lambda Physik FL2001) operating on QUI dye is used to probe the CH product. The beam is loosely focused to a ~3 mm spot by a 100 cm focal length lens at the reaction center; typical probe pulse energies are 0.5−1.5 mJ. The fluorescence from the excited molecules is imaged using a Galileo type telescope through either a 385 ± 11 nm ($v = 0$) or a 400 ± 5 nm ($v = 1$) interference filter (Corion) onto the PMT (GaAs Hamamatsu R943-02). The probe laser pulse is delayed by 4−9 μs with respect to the ablation pulse.

Analog signals from the PMT are sent to a digital storage oscilloscope (Nicolet Explorer III) and then to a laboratory computer for storage and processing. The timing sequence of the experiments is controlled by an array of pulse and delay generators allowing control of several channels with a 10 ns incremental time adjustment.

The gases used have the following stated purities: H_2 (MG Industries, 99.999%), HBr (Matheson, 99.8%), HCl (Spectra Gas, 99.99995%), and CH_3OH (Mallinckrodt, 99.9%). Liquid CH_3OD (Aldrich) was stated to be 99.8% isotopically pure. Both HBr and HCl were purified by several freeze−pump−thaw cycles at liquid nitrogen temperature to remove H_2.

III. Results and Analysis

1. Characterization of the Carbon Beam. Characterization of the atomic carbon ablation beam is necessary for several reasons. First, the ablation of graphite is known to eject a variety of carbon species in addition to $C(^3P)$. In an earlier report,[2] we have shown that in free ablation atomic carbon in its ground electronic state, $C(^3P)$, can be efficiently produced while minimizing concentrations of C_2 and C_3. This is particularly important in endothermic H-transfer reactions where the CH signal is small. In addition, C_3 fluoresces strongly in the CH (B−X) and (A−X) spectral regions,[28] which could lead to the masking of our small CH LIF signal. Ground state

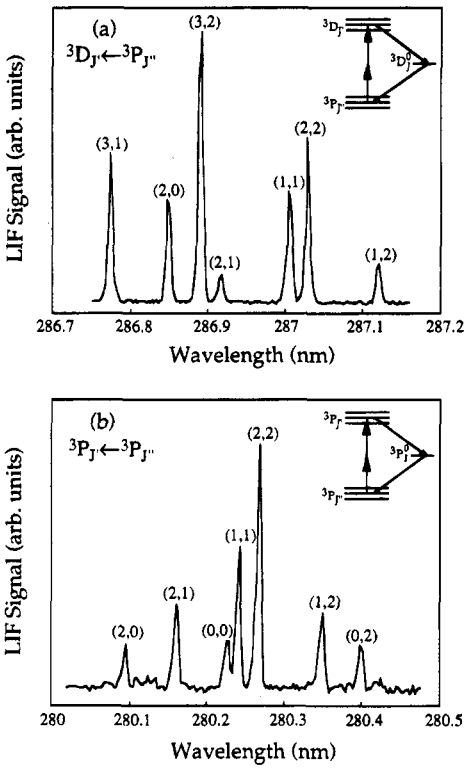

Figure 1. Two-photon LIF spectra of C(^{3}P) from 266 nm free ablation of graphite, using (a) the $^3D_{J'} \leftarrow {}^3P_{J''}$ transition at 287 nm and (b) the $^3P_{J'} \leftarrow {}^3P_{J''}$ transition. The delay between the ablation and probe pulses was 6 μs.

C(^{3}P←^{3}P,^{3}D←^{3}P), metastable C(^{1}P←^{1}D),C$_2$(D$^1\Sigma_u^+$←X$^1\Sigma_g^+$), and C$_3$(A$^1\Pi_u$←X$^1\Sigma_g^+$) are all readily detectable by LIF, and our ability to directly probe these species allows us to optimize the experimental conditions for the production of predominantly monomeric, ground state carbon.

Second, as this study examines the role of translational energy on the gas-phase dynamics of endoergic reactions of C(^{3}P), it becomes equally important to directly determine the velocity distribution within our atomic beam. Previously, we had only indirectly obtained distributions based on the time-of-flight (TOF) measurements of C$_2$, which were assumed to be similar to that of atomic carbon. In this study, however, we present direct TOF measurements of C(^{3}P) generated by both 266 and 355 nm ablation, in order to obtain a more accurate measure of the collision energy.

Detection of C(^{3}P). Two-photon excitation is a sensitive spectroscopic technique for the investigation of atoms which have their first allowed transitions in the VUV.[25,29] In this work, C(^{3}P) is detected by two-photon LIF via the $^3P_J \leftarrow {}^3P_{J''}$ transition located at ~140 nm and the $^3D_{J'} \leftarrow {}^3P_{J''}$ transition at ~143 nm. The energy level diagrams and the resulting C(^{3}P) spectra are shown in Figure 1. All the allowed transitions are clearly observed and resolved and are assigned by comparison with published frequencies.[30]

From the LIF spectra, we conclude that the spin−orbit states in C($^3P_{J=2,1,0}$) generated by free ablation are statistically populated. For a 2p3p ^{3}P ← 2p^2 ^{3}P transition, a statistical distribution is given by $(2J'' + 1)\beta_{J''-J'}$, where $\beta_{J''-J'}$ is the absorption cross section for the fine structures of the transition.[31] In the experiments, only the ratios of the populations are needed. Using the $(2J'' + 1)$ approximation only, the relative J''-state populations obtained from the diagonal $^3P \leftarrow {}^3P$ transitions are statistical, but do not agree with those obtained from the off-diagonal (2,1), (1,2), (2,0), and (0,2) transitions. Although the β values have not been determined for carbon, Hartree−Fock

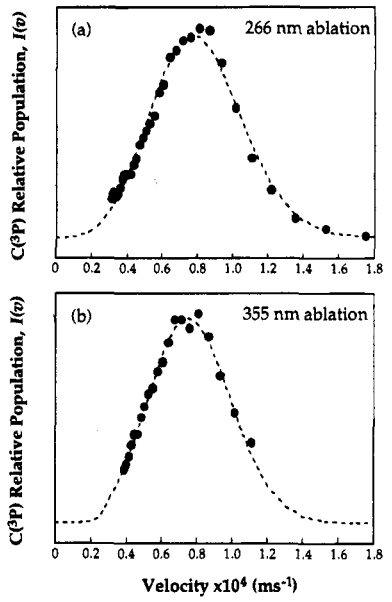

Figure 2. C(^{3}P) velocity distributions obtained for (a) 266 nm ablation (4 mJ) and (b) 355 nm ablation (10 mJ). The experimental points are represented by the filled circles. The dashed line is a nonlinear least squares fit to a shifted Maxwell−Boltzmann distribution with a peak velocity of 8000 m s^{-1} and beam translational temperatures of 21 000 and 9500 K for 266 and 355 nm ablations, respectively.

calculations have yielded values for the corresponding two-photon 2p^{3}3p ^{3}P ← 2p^4 ^{3}P transition for atomic oxygen.[31] Using the same relative $\beta_{J''-J'}$ values (assuming that the relative values are similar), the populations obtained from all observed transitions are in agreement and indicate that the J''-state populations are statistical.

C(^{3}P) Velocity and Translational Energy Distributions. As quantities measured by LIF are number densities, the experimental TOF distributions, $n(t)$, are essentially number density distributions. The TOF spectra are converted to velocity distributions, $n(v)$, using the Jacobian transformation,

$$n(v) = n(t)t^2/L$$

where t is the ablation-probe delay and L is the atomic C(^{3}P) flight distance. These distributions are then converted from number density to flux distributions, $I(v)$, employing a correction factor of L/t to account for the fact that atoms with lower velocities are preferentially detected by LIF.

For both ablation wavelengths (266 and 355 nm) and all pulse energies used, the peak of the C atom velocity distribution is at ~8000 m s^{-1}. The velocity distributions are broad, approximately 6000 m s^{-1} fwhm for 266 nm ablation, narrowing to 5000 m s^{-1} fwhm for 355 nm ablation. The distributions are also observed to narrow slightly at higher fluences.

For a more complete analysis, a shifted Maxwell−Boltzmann (MB) distribution,

$$I(v) = Av^3 \exp[-(v - v_s)^2/\alpha^2]$$

is fit to the experimental distributions using a nonlinear least-squares procedure.[1] Here, $\alpha = (2kT/m)^{1/2}$ is the width of the speed distribution as measured by a "beam-bound" observer, v is the velocity, v_s is the stream velocity of the beams, and $I(v)$ is the fractional flux at velocity v. The data and fitted curves are displayed in Figure 2. The shifted MB function also describes the velocity distribution of a supersonic molecular beam[1] and has been previously applied to characterize the velocity distributions of beams of laser-ablated material.[20,22,32]

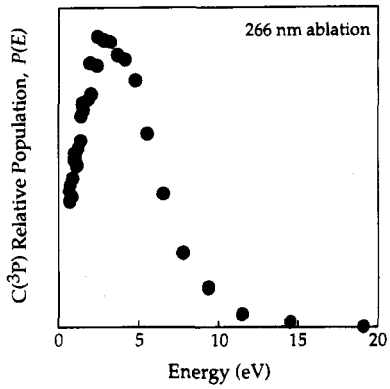

Figure 3. C(^{3}P) translational energy distribution obtained from the transformation of the TOF data as described in the text, using 266 nm ablation (4 mJ).

A simplistic physical picture is that of a dense, gaseous plume being formed by laser vaporization, followed by gradual expansion into the vacuum. Translational energy is gained both via collisions within the plume and with the bulk target, as well as from the possible photofragmentation of higher order C_n species. A random distribution of velocities given by the translational temperature, T, is thus superimposed on the stream velocity, v_s, of the expanding cloud. From the analysis of the resulting MB curves, the translational temperatures of our atomic beam generated by 266 and 355 nm ablation are 21 000 ± 4000 and 9500 ± 2000 K, respectively. Although the width of the velocity distribution obtained with 355 nm ablation is narrower, the intensity of the C(^{3}P) beam is much lower and the relative concentrations of C_2 and C_3 are higher. Thus, in the studies reported here only 266 nm ablation has been used.

Energy distributions, *n(E)*, are similarly obtained using the Jacobian transformation,

$$n(E) = n(t)t^3/mL^2$$

and converted to flux distributions, *P(E)*. Both 266 and 355 nm ablation show a maximum at approximately 3 eV with a high-energy "tail" extending beyond 10 eV. A representative plot for the 266 nm ablation used in the present experiments is given in Figure 3.

High translational energies of C_n neutrals have been previously observed from free laser ablation of graphite. Using LIF technique similar to ours, Pappas *et al.*[21] measured the TOF distributions of C_2 generated by 248 nm ablation of polycrystalline graphite. At a fluence of 2.2 J/cm^2, maximum C_2 translational energies of 12 eV were observed. Bykovskii *et al.*[22] used 1.06 μm radiation for ablation and TOF mass spectrometry for detection and characterization of carbon and metal ablation plasmas. A peak translational energy of ~2 eV was observed for atomic carbon at a fluence of 0.8 J/cm^2. Most recently, Krajnovich,[23] also using TOF mass spectrometry, conducted a detailed study of the ablation of highly oriented pyrolytic graphite (HOPG) by 248 nm radiation, at fluences of 0.3−0.7 J/cm^2. Translational energy distributions were obtained for atomic carbon, C_2 and C_3 neutrals, and showed a strong fluence dependence. For example, the mean translational energy of atomic carbon over the range of fluences investigated was observed to be 0.8−9.7 eV. The distributions were best fit to an *effusive* Maxwell−Boltzmann distribution (in contrast to this work); however, the very high translational energies observed also indicated the participation of a nonthermal process. High translational energies from free laser ablation have also been observed for several metal atomic species, including Al (~4 eV) from the ablation of Al_2O_3,[32] Cu (~4 eV) from the ablation of CuO, Zn (~1.5 eV) from the ablation of $ZnBr_2$, and Ni (~5 eV) from the ablation of NiO.[33] It appears that although high translational energies of ablated species are common, the peak energy and shape of the distributions are dependent on the source and conditions, underscoring the need for characterization.

This work has yielded a revised value for the translational energy of the atomic carbon beam. In a previous study,[2] the average translational energy was assumed to be 4.5 eV for 266 nm free ablation, based on the analysis of TOF data obtained by monitoring C_2 LIF. The values determined here are somewhat lower, but since they result from direct detection of C(^{3}P), we believe that they are more accurate. Although the discrepancy is not easily accounted for, it is possible that there are differences in the ablation mechanisms for production of the distinct species.

Center-of-Mass Collision Energy Distributions. The translational energy distribution of the atomic carbon beam can subsequently be used to calculate the center-of-mass (CM) collision energy distributions of the four reactive systems. The translational energies of the reactant molecules [H_2, HBr, HCl, CH_3OH(D)] in the molecular beam are estimated based on calculated values for a fully expanded beam.[34] The velocity of neat N_2O expanded under similar conditions has been measured before (by using a fast ionization gauge to record the difference in arrival time of the gas pulse at two different nozzle−gauge distances) and found to be approximately 700 m s^{-1}; this corresponds quite reasonably to the calculated value of 715 m s^{-1}. Using calculated values for the molecular beams, CM collision energy distributions are obtained by using the average energy of the molecular reactant, reduced mass, and the experimentally determined C atom translational energy distribution (266 nm ablation). The distributions for the C + HCl, HBr, and CH_3OH systems are fairly similar, peaking at 2 eV with a high-energy tail beyond 8 eV, while that for the C + H_2 system peaks at 0.5 eV with a high-energy tail beyond 2 eV. The noticeably lower collision energies of the C + H_2 system are due to the much lower reduced mass. It should, however, be noted that the values presented here do not take into account the molecular beam velocity spread, which would further extend the high-energy tail.

2. CH($X^2\Pi$) Internal State Distributions. The rotational distributions of CH($X^2\Pi$,v''=0) from reactions 1−4 were obtained following 266 nm ablation from the LIF spectra of the $B^2\Sigma^- \leftarrow X^2\Pi$ transition. The experimental conditions and the relative collision energies are discussed in section III.1. Figure 4 displays a typical CH($B^2\Sigma^-$−$X^2\Pi$) LIF spectrum obtained from the reaction of C(^{3}P) with HBr showing the entire R branch and portions of the Q and P branches. Small CH signals were obtained for all the endoergic reactions investigated, as compared for example to the much larger CN($B^2\Sigma$←$X^2\Sigma$) signals obtained from the exothermic C(^{3}P) + N_2O reaction.[2,3] Taking into account that the electronic transition strength of CN is approximately 4-fold greater than that of CH (0.817 and 0.212 au, respectively),[35] the CH signals are about a factor of 10 smaller. However, since CN is produced in many more rovibrational states,[3] the actual probability of production of CH is much smaller. Signals from C_3 LIF and background emission from the ablation contribute to the poor signal-to-noise (S/N) ratios; the best S/N ratios are achieved at an ablation−probe delay of 6 μs, near the peak of the atomic carbon TOF data. The use of shorter delay times was complicated by the interference from background radiation from the free ablation which peaks at earlier times.

Although the most endoergic of the reactions examined, the

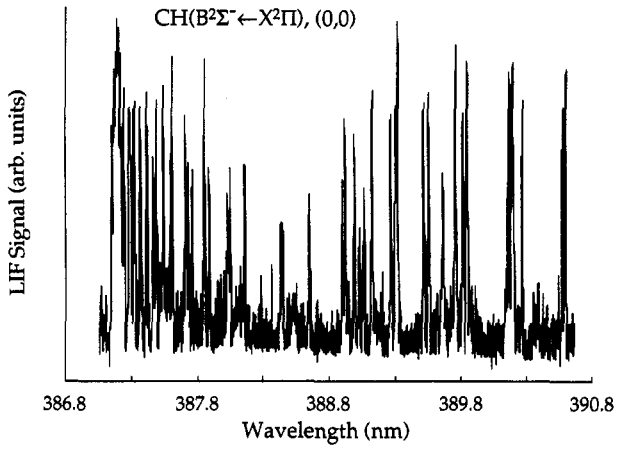

Figure 4. CH ($B^2\Sigma^- \leftarrow X^2\Pi$) (0,0) LIF spectrum showing the entire R branch and portions of the Q and P branches, obtained in the reaction of C(^{3}P) with HBr. The atomic carbon beam was generated by 266 nm free ablation (4 mJ). The HBr beam was neat, with a stagnation pressure of 760 Torr. The delay between the ablation and probe pulses was 7 μs.

strongest CH LIF signals were observed from the reaction of C(^{3}P) with H_2. This is attributed both to the fact that twice as much CH can be produced here as compared with the C(^{3}P) + hydrogen halide reactions, and to the absence of other competing reaction pathways which would yield other products (e.g., CCl, CBr). All CH spectra were obtained under saturation conditions at a probe energy fluence of ~10 mJ cm^{-2}. Detailed measurements have determined the onset of saturation to be 0.06 mJ cm^{-2}, with near-saturation conditions being achieved at 0.6 mJ cm^{-2}.[7]

Relative CH rotational populations, $n(N'')$, were derived from measured peak heights of the B ← X transition assuming complete saturation and using

$$n(N'') = I(N'')(g'' + g')/g'$$

where $I(N'')$ is the rotational line intensity and g' and g'' are the degeneracies of the upper and lower states, respectively. Figure 5 shows the R-branch level populations for both spin–orbit states obtained from the analysis of the reactions of C(^{3}P) with H_2, HBr, HCl, and CH_3OH. These distributions are the result of averaging over the populations obtained from several scans. This is necessary because momentary fluctuations in the ablation conditions can lead to momentary changes in the C-beam intensity, which in turn can randomly enhance or diminish CH spectral features. Analysis of the Q branch intensities has yielded similar distributions. All rotational distributions are rather similar, peaking at ~$N'' = 7$ and decreasing substantially by $N'' = 14$. The rotational distributions were unaffected by reducing the stagnation pressure (and hence the background chamber pressure) and by increasing the distance of the molecular reactant nozzle from the reaction center. The distributions did not change when varying the delay between the ablation and probe lasers from 4 to 9 μs. In addition, changing the ablation wavelength to 355 nm, at delays corresponding to the peak of the C(^{3}P) distribution, also did not alter the CH distributions.

The rotational distributions can be well described by temperatures of 2200 ± 200, 2000 ± 200, and 2200 ± 200 K for the reactions of carbon with HCl, HBr, and CH_3OH, respectively; a lower temperature of 1500 ± 100 K is obtained in the reaction with H_2 from the slightly narrower CH distribution. These temperatures correspond to an average energy in CH rotation of ~0.13 eV from the reaction with H_2 and of ~0.19 eV from reactions with HCl, HBr, and CH_3OH. Because free

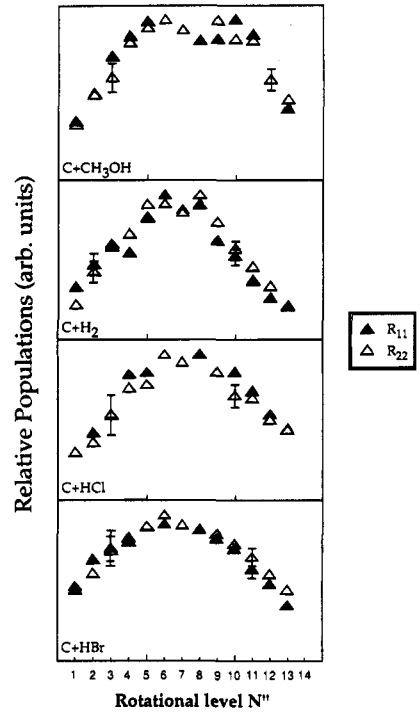

Figure 5. CH($X^2\Pi, v=0$) rotational distributions obtained from the reactions of C(^{3}P) with CH_3OH, H_2, HCl, and HBr as indicated on the respective plots. Filled and empty triangles correspond to the R branches of the F_1 and F_2 spin–orbit states, respectively. The data points plotted are the average of several CH distributions obtained for each reaction. Rotational lines were normalized as described in the text. The data were obtained under the typical experimental conditions described in section II.

ablation produces a broad distribution of collision energies, it is difficult to determine the fractional energy partitioned into CH rotation as a function of collision energy. For example, in the reaction of C with H_2, which is 1.00 eV endoergic, the peak collison energy is only 0.5 eV; however, comparatively strong CH signals are observed, which manifest the contributions from the high-energy "tail" that extends beyond 2 eV. No vibrational excitation of the CH diatomic product is observed in the reactions investigated in this study, and the spin–orbit states are equally populated.

The rotational distribution for the reaction of C(^{3}P) with CH_3OH is observed to be slightly broader than those for the reactions with H_2, HBr, and HCl. This may reflect the existence of two reactive sites, i.e., the methyl and the hydroxyl sites. To investigate the possibility of participation of the stronger O–H bond, we examined the reaction of C(^{3}P) with CH_3OD in an attempt to detect CD($X^2\Pi$). The B ← X transition in CD is in the same spectral region as that of the CH B ← X transition with the CD bandhead appearing slightly earlier at around 386.4 nm;[36] however, the transition is not nearly as well characterized in the literature as that of CH. To ensure our ability to identify CD, CD_3I was photolyzed by two-photon absorption at 266 nm, and the B ← X transition of CD was recorded. Assignments are subsequently based both on comparisons with CD photolysis line positions and with published data.[33] Figure 6 shows the LIF spectrum obtained for the reaction of C(^{3}P) with CH_3OD. Although the reaction channel for O–H abstraction is ~0.4 eV more endothermic than that for C–H abstraction, several peaks clearly assignable to CD($^2\Pi$) are observed before the CH R-branch bandhead appears at 387.14 nm. Even though the CD signal is smaller than that of the CH, recall that there are three H atoms for every D atom in CH_3OD. The CH rotational distributions are very similar to those obtained from the other reactions studied; however, we were unable to extract the CD

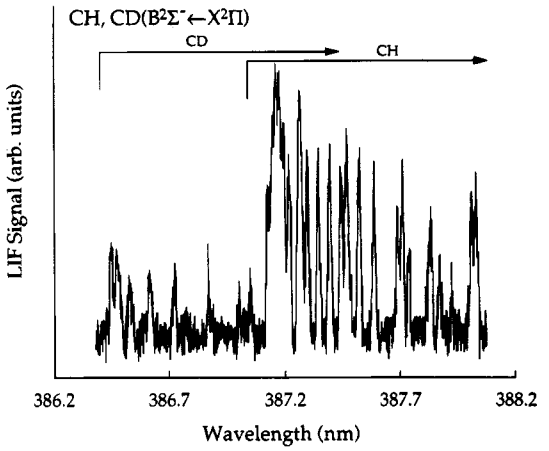

Figure 6. CH and CD ($B^2\Sigma^-$←$X^2\Pi$) LIF spectra obtained from the reaction of C(^{3}P) with CH_3OD. Several peaks assignable to CD are observed before the CH R-branch bandhead at 387.14 nm. The atomic carbon beam was generated by 266 nm free ablation (4 mJ). A 50% CH_3OD/He beam was used with a stagnation pressure of 760 Torr. The delay between the ablation and probe laser was 6 μs.

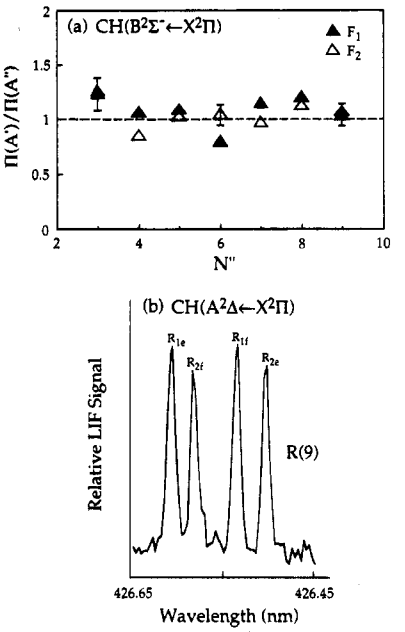

Figure 7. (a) CH($X^2\Pi$) Λ-doublet population ratios obtained via the $B^2\Sigma^-$ ← $X^2\Pi$ transition in the C(^{3}P) + H_2 reaction. Filled and empty triangles correspond to the F_1 and F_2 spin−orbit components, respectively. (b) LIF spectrum of the R(9) lines obtained via the $A^2\Delta$ ← $X^2\Pi$ transition under the same condition as in (a). The 1e and 2f lines are associated with the in-plane Π(A′) component, and the 2e and 1f lines are associated with the out-of-plane Π(A″) component. The H_2 beam was neat with a stagnation pressure of 760 Torr. The delay between the ablation and probe pulses was 5 μs.

rotational distributions due to the rotational line overlap of the CD peaks observed and the masking of any CD signal obtained in the CH spectral region. A similar broadening in the rotational distribution of product OH obtained from the reaction of O(^{3}P) + C_2H_5OH (when compared to the OH distributions obtained from reactions of O(^{3}P) with other organic molecules) was also observed and ascribed to contributions from both methyl and hydroxyl H-transfer sites.[37]

3. CH($X^2\Pi$) Λ-Doublet Populations. In the limit of Hund's case b, the populations of the Λ-doublet components of electronic states of radicals in Π states yield information on the preferential orientation of the unpaired π-orbital with respect to the plane of rotation of the diatom.[38,39] For reactions proceeding via a collision complex, the Λ-doublet propensities may indicate whether the unpaired electron originates from an in-plane, Π(A′), or out-of-plane, Π(A″), orbital in the intermediate. In CH($X^2\Pi$), the Hund's case b limit is approached already by $N'' \sim 2$,[38] and therefore, Λ-doublet propensities can be easily obtained.

To determine the Λ-doublet propensities in the CH product of the reactions studied using the $B^2\Sigma^-$ ← $X^2\Pi$ transition, a quantitative comparison between the rotational level populations of the Q- vs P- and R-branch lines is necessary. Q and P/R lines are associated with the Π(A′) and Π(A″) Λ-doublet components, respectively.[7,38,39] Assuming saturation and neglecting polarization, in a $^2\Sigma^-$ ← $^2\Pi$ transition

$$n[J'',\Pi(A'')]/n[J'',\Pi(A')] = CI_{P,R}(J'')/I_Q(J'')$$

where $n[J'',\Pi(A'',A')]$ is the population of the Π(A″) or Π(A′) Λ-doublet components of the J'' rotational level. $I_{P,R}(J'')$ is the intensity of the P(J'') or R(J'') line, $I_Q(J'')$ is the intensity of the Q(J'') line, and

$$C = {}^1/_2[(2J'' + 1)/(2J''_{P,R} + 1) + 1]$$

Recall that $J'' = N'' + {}^1/_2$ and $N'' - {}^1/_2$ for F_1 and F_2 states, respectively.

The populations of the two CH($X^2\Pi$) Λ-doublet components for the reactions studied have been obtained for $N'' = 3-10$. No significant propensities for either component are observed. The results for the reaction of C(^{3}P) with H_2 are displayed in Figure 7a. Corrections for the degree of electron alignment (DEA) were considered unnecessary,[38] as any correction factor will be within our error estimate. As an additional check, a direct measurement of the Λ-doublet populations was conducted for the reaction with H_2 using the R(9) lines of the CH $A^2\Delta$ ← $X^2\Pi$ (0,0) transition. For the higher rotational levels in CH($X^2\Pi$), the Λ-doublets, as well as the spin−orbit components of each branch line, are well separated.[27,40] The data obtained show conclusively that the two Λ-doublet components are equally populated (Figure 7b). Here, the F_{1e} and F_{2f} wave functions correspond to the Π(A′) Λ-doublet component, while the F_{1f} and F_{2e} correspond to the Π(A″) component. Note also that the F_1 and F_2 states of the same N'' correspond to J'' states which differ by 1.

IV. Discussion

1. Reactions Leading to CH($X^2\Pi$) Formation. The CH LIF signals reported here, which result from endoergic reactions, are small, and therefore it is important to ascertain that the reaction of C(^{3}P) with the reactant molecules is indeed the main source of the observed CH($X^2\Pi$). When the observed species is a minor product, even small contributions from other processes (e.g., reactive contaminants and photolytic processes) can interfere, and their role, if any, has to be assessed.

Although not observed in previous studies, metastable atomic carbon, C(^{1}D), which is 1.26 eV higher in energy than the ground ^{3}P state, is a possible byproduct of the ablation process, and its reactions with the reactants studied here are exoergic. Even in minute quantities, C(^{1}D), which reacts fast [$(k = (2.6 \pm 0.3) \times 10^{-10}$ cm^3 molecule^{-1} s^{-1}][41] and exothermically [$\Delta H = -0.26$ eV] with H_2 to produce CH($X^2\Pi$), could significantly contribute to our observed signal. Since the CH rotational distribution and the Λ-doublet ratios obtained with H_2 in this study are similar to those produced in the C(^{1}D) + H_2 reaction,[7-10] it is essential to eliminate C(^{1}D) as a source of the observed CH. Obviously, however, because of both the high collision energies employed in this study and our good sensitiv-

ity of CH detection, the endoergic channel for reaction with C(^{3}P) is accessible and observable.

Several experiments were conducted to distinguish between C(^{3}P) and C(^{1}D) as the source of CH. First, we attempted to directly detect C(^{1}D) via the LIF of the $^1P_1 \leftarrow {}^1D_2$ transition.[25b] Although C(^{1}D) can be readily observed using two-photon LIF detection, it was not observed in the detection region from the laser ablation of graphite. In addition, a study by Monchicourt[24] which monitored the fluorescence from excited carbon species within the ablation plume itself (before collisional quenching and expansion) also did not observe any singlet states, identifying only excited triplet states as the emitting atomic carbon species. On the basis of the observed S/N, assuming equal transition probabilities for the two states and recalling that the ^{3}P population is partitioned among several J'' states as opposed to one J'' state for ^{1}D, we can estimate an upper limit of $\leq 0.1\%$ of C(^{1}D) relative to C(^{3}P) in the beam. In the second experiment, we attempted to detect CH from the reaction with H_2 with the carbon beam generated by ablation and seeding in He. In the seeded mode, the laser-ablated material is entrained in a carrier gas prior to expansion, which gives a narrow velocity distribution and allows kinetic energy control of the carbon beam. A more detailed description of generating the seeded beam has been given elsewhere.[2] In this experiment, the ablated carbon atoms were entrained in He at a backing pressure of 8 atm, lowering the CM collision energy with H_2 to 0.15 ± 0.02 eV.[2] Thus, any signal observed could only result from the exoergic reaction with C(^{1}D). No CH was detected; however, C(^{1}D) formed in the ablated beam may also be removed via collisional quenching by helium atoms before reaching the interaction region. Although the quenching efficiency of C(^{1}D) by helium is quite low ($k < 3 \times 10^{-16}$ cm^3 molecule^{-1} s^{-1}),[42] some quenching can still occur before the expansion is complete. Also, the greater production of C_3 in the seeded beam and the lower density of atomic carbon may mask a small CH signal. However, a qualitative comparison of the ratio of the CN product signals obtained in the C(^{3}P) + N_2O reaction using free and seeded ablation of graphite indicates that had there been a CH signal originating from the C(^{1}D) + H_2 reaction, it could be observed in the seeded mode above the C_3 background.

Indirect evidence that translational energy can promote H-transfer reactions of atomic carbon comes from the observation of a CH signal in reactions which are endoergic for both C(^{3}P) and C(^{1}D). For example, with C_2H_2 as the reactant, we observe CH signals comparable in magnitude to those observed in the reaction with H_2, even though the C(^{1}D) channel is endoergic as well ($\Delta H = 0.8$ eV). These results, combined with the other evidence presented above, lead us to believe that reactions of C(^{3}P) are responsible for the CH signals observed in this study.

Other possible sources of CH($^2\Pi$) have also been investigated. In addition to C(^{3}P), both C_2 and C_3 molecules are minor components of our ablation beam and can react exoergically with the H-containing reactants to form C_2H and C_3H, respectively. CH could possibly be formed from these products via multiphoton dissociation by the probe laser. However, this would necessitate the breaking of a C=C double bond or a C≡C triple bond, which requires at least a three-photon absorption process and is considered unlikely. No product CH was detected on replacing H−X reactants with He, suggesting that both carbon and the H donor are required. In addition, in the case of CH_3OH, CH signals were observed to be quite sensitive to the concentration of the reactant in the seeded beam. Multiphoton dissociation of molecular reactants by either probe or ablation lasers was also investigated by suppressing C(^{3}P) formation while continuing to scan the probe laser; no CH was detected. As a result of these investigations, we conclude that C(^{3}P) is the major reactant leading to the formation of CH($X^2\Pi$).

2. Energy Disposal and Reaction Mechanisms. As discussed in section II, the observed rotational distributions of the CH($X^2\Pi$) product are rather similar for all the reactions reported here and can be assigned temperatures ranging from 1500 to 2200 K (or average energy in rotation of 0.13−0.19 eV). No $v = 1$ signal could be confidently identified above the small C_3 LIF background. The similarity in the rotational distributions is rather surprising at first glance, considering the differences in the reduced mass of the collision systems, which result in a much smaller CM collision energy for the reaction with hydrogen. It is possible that the rotational distributions are determined by dynamical constraints and do not depend strongly on the collision energy. Also, the dependence of the reaction cross sections on collision energy is yet unknown, and in the present method of C(^{3}P) production, which results in a broad distribution of collision energies, the relative contributions of the different collision energies to the observed signal cannot be assessed. Thus, the fraction of energy channeled into product rotation cannot be determined. For example, if the reactions proceed via insertion on an attractive potential energy surface (see below), too high collision energies may cause a decrease in cross section, since the probability of capture into the reactive well may be lower.

There is only one reaction of C(^{3}P) to which our results can be compared—the exoergic reaction with HI. In this reaction, CH in both $v = 0$ and $v = 1$ has been observed,[6] but no rotational distributions have been reported, since the system was relaxed. Typically, inversion in the vibrational populations of product molecules is a characteristic feature of the product distributions for light atom-transfer reactions;[43] for example, high vibrational excitation has been observed in many exothermic H atom-transfer reactions of O(^{3}P)[44-46] (see below).

The reaction of C(^{1}D) with H_2 has been studied by several groups.[8-10] The rotational distribution and spin−orbit ratios of the CH products are rather similar to those observed here for the reaction of C(^{3}P). There is still some controversy regarding the Λ-doublet propensities; either no preference[7] or a small preference for the in-plane component has been reported.[8,10] The C(^{1}D) + HCl reaction has also been studied and shows no Λ-doublet and spin−orbit preferences.[7] The rotational distribution is hotter than the one reported here, but contributions from other reactants generated in the photodissociation of the C(^{1}D) precursor, C_3O_2, which yield CH at high rotational states, could not be conclusively ruled out.[7]

In a previous publication on the reactions of C(^{1}D), we suggested that if carbene insertion intermediates are involved, then several of their low-lying singlet and triplet surfaces may participate, thus rationalizing the absence of significant Λ-doublet preferences in the CH product.[7] Several theoretical studies on the C(^{3}P) + H_2 reaction support this suggestion.[12,15,16]

Using ab initio calculations, Blint and Newton determined that H atom abstraction by C(^{3}P) follows an axial $C_{\infty v}$ least-energy path along the $^3\Pi$ surface, with a rather late barrier of 34.7 kcal mol^{-1} (1.5 eV).[15] A later study by Harding *et al.* also reported a similar barrier to linear abstraction of 29.6 kcal mol^{-1}(1.3 eV).[12] Insertion via a C_{2v} perpendicular path along the $^3B_1$ surface was found to involve a substantial barrier of 91.7 kcal mol^{-1} (4.0 eV). However, starting with C(^{3}P) and H_2, at large separations there are three degenerate triplet states for a C_{2v} orientation. (The $^3B_2$ surface is the highest of the three and will be ignored.) At larger separations the $^3A_2$ state

is lower in energy owing to a dative bonding interaction between the empty carbon p orbital and H_2.[12] Thus, in the vicinity of the $^3B_1$ barrier, the $^3A_2$ state (which lies at much higher energies at the equilibrium CH_2 geometry) has a much lower energy. However, at small separations, the $^3B_1$ state will drop below the other two. In C_s approaches, these two surfaces interact via a conical intersection, and the avoided crossing lowers the barrier substantially.[12,15,16] Most recently, Harding *et al.* reported theoretical studies on the H + CH → C + H_2 and C + H_2 → CH_2 reactions using ab initio global ground state potential energy surface (PES) for CH_2.[12] They again found that the latter reaction proceeds via an insertion mechanism facilitated by a crossing with the $^3A_2$ surface, but they also found that the barrier to insertion is eliminated and that the CH_2 intermediate lives for ~20 ps at thermal energies. In addition, no barriers are expected in the exit channel.[12] Thus, a barrierless insertion route is available for the C(^{3}P) reaction with H_2. This mechanism may explain the rather high rates measured for the C(^{3}P) + H_2 reaction at high temperatures.[47]

In the CH_2 radical, the low-lying singlet and triplet states are known to be strongly mixed,[48-52] and thus it is possible that the reactions of C(^{3}P) and C(^{1}D) with H_2 proceed via the same intermediate, giving rise to similar product energy distributions. In fact, studies of the CH_2 radical have suggested that owing to these strong mixings, the kinetics of singlet and triplet methylene cannot be treated separately.[49,50] The absence of Λ-doublet preferences can be explained, as in the case of the C(^{1}D) reactions,[7] by the participation of triplet and/or singlet states of B_1 symmetry. These states have unpaired electrons in a b_1 orbital, which is perpendicular to the CH_2 plane, and therefore, following bond fission and electron reorganization, the CH product may be formed in both Π(A′) and Π(A″) Λ-doublet states. Thus, no specific propensity rules can be predicted for these mixed states.

Although no calculations are available for the reactions of C(^{3}P) with HCl and HBr, the corresponding carbene intermediates are expected to have much stronger singlet−triplet couplings than in CH_2, and surface crossings similar to those identified for the C(^{3}P) + H_2 reaction may lower the barrier to insertion. For the HCCl intermediate, for example, ab initio calculations give a singlet−triplet separation of 1900 cm^{-1} (0.2 eV),[53] and the measured origin of the first excited singlet state, ^{1}A″, is at ~12 000 cm^{-1} (1.5 eV) above the singlet ground state.[54]

The reaction of C(^{3}P) with CH_3OD exhibits no site specificity, yielding both CH and CD products. It is premature to speculate whether two insertion routes are open or whether both insertion and abstraction pathways are important. Both theoretical calculations and studies on the dependences of each channel on translational energy are required to resolve these issues. Since it was not possible to vary the C(^{3}P) translational energy by varying the fluence of the ablation laser, we plan to use other precursor materials in the ablation in an attempt to vary the translational energy. Also, reactions in which the CH or OH stretch vibrations are excited may exhibit additional enhancements and provide further clues regarding mechanisms.

The theoretical calculations and the similarity of the results obtained in the C(^{1}D) and C(^{3}P) reactions with H_2 suggest that an insertion mechanism is important for both. If, indeed, insertion is the primary mechanism for other endoergic H-transfer reactions of C(^{3}P) as well, then it stands in contrast to the corresponding reactions of O(^{3}P) which are thought to proceed via an abstraction mechanism on the lowest triplet surface correlating with the reactants.[44,45,55] These reactions are usually characterized by early barriers in the entrance channel and result in high vibrational excitation in the OH product.[43a] This is typical of heavy−light−heavy (HLH′) reactions in which the light H atom is transferred at relatively large internuclear distances.[1] The "corner cutting" trajectories typically cause translational energy to be channeled preferentially into product vibration.[43b,c] Although the collision energy available in the present studies is sufficient in all cases except H_2 for vibrational excitation of the CH product, no significant population in v = 1 has been observed, supporting the suggestion that the mechanisms of the O(^{3}P) and C(^{3}P) H-transfer reactions are different. It should also be noted that, at increased translational energy, the relative contributions from insertion and abstraction reactions may change and that the CH excitations produced via either mechanism are likely to depend on translational energy. Without more support from theory and measurements at different translational energies, it is imprudent at this point to further speculate on these issues.

V. Summary

A beam source of hyperthermal C(^{3}P) based on 266 nm laser ablation of graphite is described and characterized. The source yields directional beams of carbon with a peak velocity of ~8000 m s^{-1}, a broad velocity distribution with fwhm ~6000 m s^{-1}, and a tail extending toward higher velocities. The conditions in the source can be optimized to generate predominantly C(^{3}P) with only minor contaminations from C_2 and C_3. The source is reliable and produces rather high intensities of C(^{3}P). Its main disadvantages are its broad velocity distribution and the inability to change the peak velocity.

Using this source, the endoergic reactions of C(^{3}P) with H_2, HCl, HBr, and CH_3OH(D) have been studied. CH is found as a product in all the reactions. It is produced predominantly in v = 0 with a rotational distribution that can be assigned temperatures of 1500−2200 K, depending on the molecular reactant. The spin−orbit and Λ-doublet components are equally populated. Comparisons with the reaction of C(^{1}D) with H_2 reveal that the CH rotational distributions and spin−orbit and Λ-doublet ratios are quite similar for both reactions. On the basis of theoretical calculations and the known electronic states of the methylene intermediate, it is suggested that the reaction of C(^{3}P) with H_2 proceeds via insertion and involves a short-lived carbene intermediate. Calculations show that surface crossings between low-lying triplet surfaces serve to reduce activation barriers to insertion,[12] and the known mixings between singlet and triplet states in CH_2 are apparently responsible for the similar CH product state distributions obtained in the reactions of C(^{3}P) and C(^{1}D) and for the absence of Λ-doublet preferences. An insertion mechanism may also be important in other H-transfer reactions.

Since these are the first results reporting nascent product distributions from endoergic H-transfer reactions of C(^{3}P), more work is evidently needed. In progress are studies of reactions with other H-containing molecules, as well as reactions with deuterated and partially deuterated reactants. Laser ablation of substrates other than graphite is implemented in an attempt to produce C(^{3}P) with different translational energies. Theoretical calculations on the reactions of C(^{3}P) with H-containing molecules of the type described in ref 12 are needed to determine the influence of surface crossings and collision energies on product branching ratios and state distributions.

Acknowledgment. The authors thank Dr. David Scott and Dr. Fiona Winterbottom for their invaluable help in the development of the carbon source, Dr. Craig Bieler for assistance with data analysis, and Dr. Larry Harding for helpful discussions

regarding the mechanism of carbon reactions with hydrogen. This study was supported by the director, Office of Energy Research, Office of Basic Energy Sciences, Chemical Sciences Division of the U.S. Department of Energy, under Grant DEFG03-88ER13959.

References and Notes

(1) Levine, R. D.; Bernstein, R. B. *Molecular Reaction Dynamics and Chemical Reactivity*; Oxford University Press: New York, 1987.

(2) Scott, D. C.; Winterbottom, F.; Scholefield, M. R.; Goyal, S.; Reisler, H. *Chem. Phys. Lett.* **1994**, *222*, 471.

(3) Reid, S. A.; Winterbottom, F.; Scott, D. C.; de Juan, J.; Reisler, H. *Chem. Phys. Lett.* **1992**, *189*, 430.

(4) (a) Jackson, W. M.; Bengre, C. N.; Halpern, J. B. *J. Photochem.* **1980**, *13*, 319. (b) Krause, H. F. *Chem. Phys. Lett.* **1981**, *78*, 78; **1981**, *83*, 165. (c) Sekiya, H.; Tsuji, M.; Nishimura, Y. *J. Chem. Phys.* **1986**, *84*, 3739.

(5) (a) Costes, M.; Naulin, C.; Dorthe, G.; Houdden, Z. *Laser Chem.* **1990**, *10*, 367. (b) Costes, M.; Naulin, C.; Dorthe, G. *Astron. Astrophys.* **1990**, *232*, 270. (c) Naulin, C.; Costes, M.; Dorthe, G. *Chem. Phys.* **1991**, *153*, 519.

(6) Nishiyama, N.; Sekiya, H.; Nishimura, Y. *J. Chem. Phys.* **1986**, *84*, 5213.

(7) Scott, D. C.; de Juan, J.; Robie, D. C.; Schwartz-Lavi, D.; Reisler, H. *J. Phys. Chem.* **1992**, *96*, 2509.

(8) (a) Jursich, G. M.; Wiesenfeld, J. R. *Chem. Phys. Lett.* **1984**, *110*, 14. (b) Jursich, G. M.; Wiesenfeld, J. R. *J. Chem. Phys.* **1985**, *83*, 910.

(9) Fisher, W. H.; Carrington, T.; Sadowski, C. M.; Dugan, C. H. *Chem. Phys.* **1985**, *97*, 433.

(10) Mikulecky, K.; Gericke, K.-H. *J. Chem. Phys.* **1993**, *98*, 1244.

(11) Gaydon, A. G. *The Spectroscopy of Flames*, 2nd ed.; Chapman and Hall: London, 1974.

(12) Harding, L. B. ; Guadagnini R.; Schatz, G. C. *J. Phys. Chem.* **1993**, *97*, 5472.

(13) For reviews, see: (a) Mackay, C. In *Carbenes*; Moss, R. A., Jones, M., Eds.; Wiley and Sons: New York, 1975; Vol. II. (b) Shevlin, P. B. In *Reactive Intermediates*; Abramovich, R. A., Ed.; Plenum: New York, 1980; Vol. I.

(14) The energetics of the reactions are calculated for ground state reactants and products by using heats of formation taken from: (a) Okabe, H. *Photochemistry of Small Molecules*; Wiley and Sons: New York, 1978. (b) Benson, S. W. *Thermochemical Kinetics*; Wiley and Sons: New York, 1976. (c) Chase, M. W., Jr.; Davies, C. A.; Downey, J. R., Jr.; Frurip, D. J.; McDonald, R. A.; Syverud, A. N. *JANAF Thermochemical Tables*, 3d ed., Part I; *J. Phys. Chem. Ref. Data* **1985**, *14* (Suppl. 1).

(15) Blint, R. J.; Newton, M. D. *Chem. Phys. Lett.* **1975**, *32*, 178.

(16) Harding, L. B. *J. Phys. Chem.* **1983**, *87*, 441.

(17) Alagia, M.; Balucani, N.; Cassavecchia, P.; Stranges, D.; Volpi, G. G. *J. Chem. Soc., Faraday Trans.* **1995**, *91*, 575.

(18) Costes, M.; Naulin, C.; Dorthe, G.; Daleau, G.; Joussot-Dubien, J.; Lalaude, C.; Vinckert, M.; Destor, A.; Vaucamps, C.; Nouchi, G. *J. Phys. E* **1989**, *22*, 1017.

(19) Herman, I. P. *Chem. Rev.* **1989**, *89*, 1323.

(20) (a) Dreyfus, R. W.; Kelly, R.; Walkup, R. E. *Nucl. Instrum. Methods B* **1987**, *23*, 557. (b) Dreyfus, R. W.; Kelly, R.; Walkup, R. E.; Srinivasan, R. *SPIE Excimer Laser Opt.* **1986**, *710*, 46.

(21) Pappas, D. L.; Saenger, K. L.; Cuomo, J. J.; Walkup R. W. *J. Appl. Phys.* **1992**, *72*, 3966.

(22) Bykovskii, Yu. A.; Sil'nov, S. M.; Sotnichenko, E. A.; Shestakov, B. A. *Sov. Phys. JETP* **1987**, *66*, 285.

(23) Krajnovich, D. J. *J. Chem. Phys.* **1995**, *102*, 726.

(24) Monchicourt, P. *Phys. Rev. Lett.* **1991**, *66*, 1430.

(25) (a) Bergstrom, H.; Hallstadius, H.; Lundberg, H.; Persson, A. *Chem Phys. Lett.* **1989**, *155*, 27. (b) Das, P.; Ondrey, G.; van Veen, N.; Bersohn, R. *J. Chem. Phys.* **1983**, *79*, 724.

(26) (a) Moore, C. E.; Broida, H. P. *J. Res. Natl. Bur. Stand.* **1959**, *63A*, 19. (b) Gerö, L. *Z. Phys.* **1941**, *118*, 27. (c) Herzberg, G.; Johns, J. W. C. *Astrophys. J.* **1969**, *158*, 397.

(27) Ball, S. M.; Hancock, G.; Heal, M. R. *J. Chem. Soc., Fraraday Trans.* **1994**, *90*, 1467.

(28) Gausset, L.; Herzberg, G.; Lagerqvist, A.; Rosen, B. *Astrophys. J.* **1965**, *142*, 45.

(29) Brewer, P.; van Veen, N.; Bersohn, R. *Chem Phys. Lett.* **1982**, *91*, 126.

(30) Moore, C. E. Atomic Energy Levels, NBS Circular 467.

(31) Pindzola, M. *Phys. Rev. A* **1978**, *17*, 17.

(32) Marcier, M.; Fajardo, M. E. *Appl. Phys. Lett.* **1994**, *65*, 159.

(33) Thiem, T. L.; Watson, L. R.; Dressler, R. A.; Salter, R. H.; Murad, E. *J. Phys. Chem.* **1994**, *98*, 11931.

(34) Kolodney, E.; Amirav, A. *Chem. Phys.* **1983**, *82*, 269.

(35) (a) Danylewych, L. L.; Nicholls, R. W. *Proc. R. Soc. London, A* **1978**, *360*, 557. (b) Hinze, J.; Lie, G. C.; Liu, B. *Astrophys. J.* **1975**, *196*, 621.

(36) Gerö, L. *Z. Phys.* **1941**, *117*, 709.

(37) Dutton, N. J.; Fletcher, I. W.; Whitehead, J. C. *J. Phys. Chem.* **1985**, *89*, 569.

(38) Andresen, P.; Rothe, E. W. *J. Chem. Phys.* **1985**, *82*, 3634.

(39) Alexander, M. H.; *et al. J. Chem. Phys.* **1988**, *89*, 1749 and references therein.

(40) Bernath, P. F.; Brazier, C. R.; Olsen, T.; Hailey, R.; Fernando, W. T. M. L.; Woods, C.; Wardwick, J. L. *J. Mol. Spectrosc.* **1991**, *147*, 16.

(41) Husain, D.; Kirsch, L. J. *Chem. Phys. Lett.* **1971**, *8*, 543.

(42) Hussain, D.; Norris, P. E. *J. Chem. Soc. Faraday Discuss.* **1979**, *67*, 273.

(43) (a) Polanyi, J. C. *Acc. Chem. Res.* **1972**, *5*, 161. (b) Polanyi, J. C.; Schreiber, J. L. In *Physical Chemistry, an Advanced Treatise*; Jost, W., Ed.; Academic: New York, 1974; Vol. 6A, p 383. (c) Parr, C. A.; Polanyi, J. C.; Wong, W. H. *J. Chem. Phys.* **1973**, *58*, 5.

(44) (a) Andresen, P.; Luntz, A. C. *J. Chem. Phys.* **1980**, *72*, 5842. (b) Kleinemanns, K.; Luntz, A. C. *J. Chem. Phys.* **1982**, *77*, 3537.

(45) McKendrick, K. G.; Rakestraw, D. J.; Zhang, R.; Zare, R. N. *J. Phys. Chem.* **1988**, *92*, 5530.

(46) Zhang, R.; van der Zande, W. J.; Bronikowski, M. J.; Zare, R. N. *J. Chem. Phys.* **1991**, *94*, 2704.

(47) (a) Dean, A. J.; Davidson, D. F.; Hanson, R. K. *J. Phys. Chem.* **1991**, *95*, 183. (b) Braun, W.; Bass, A. M.; Davis, D. D.; Simmons, J. D. *Proc. R. Soc. London, A* **1969**, *312*, 417. (c) Peeters, J.; Vinckier, C. *Proc. Symp. (Int.) Combust.* **1974**, *15*, 969.

(48) Gaspar, P. P.; Hammond, G. S. In *Carbenes*; Moss, R. A., Jones, M. Jr., Eds.; Wiley and Sons: New York, 1975; Vol. II, p 204.

(49) Petek, H.; Nesbitt, D. J.; Moore, C. B.; Birss, F. W.; Ramsay, D. A. *J. Chem. Phys.* **1987**, *86*, 1189.

(50) Petek, H.; Nesbitt, D. J.; Darwin, D. C.; Moore, C. B. *J. Chem. Phys.* **1987**, *86*, 1172.

(51) Shavitt, I. *Tetrahedron* **1985**, *41*, 1531.

(52) Schaefer, H. F., III. *Science* **1986**, *231*, 1100.

(53) (a) Irikura, K. K.; Goddard, W. A., III; Beauchamp, J. L. *J. Am. Chem. Soc.* **1992**, *114*, 48. (b) Scuseria, G. E.; Durán, M.; Maclagan, G. A. R.; Schaefer, H. F., III. *J. Am. Chem. Soc.* **1986**, *108*, 3248.

(54) Jacox, M. E. *J. Phys. Chem. Ref. Data* **1988**, *17*, 269.

(55) Luntz, A. C. *J. Chem. Phys.* **1980**, *73*, 1172.

JP9513071